

3-1-1992

# Design Curves for Transient Heat Flow in Semiconductor Devices

James A. Cooper, Jr.

*Purdue University School of Electrical Engineering*

Follow this and additional works at: <http://docs.lib.purdue.edu/ecetr>

---

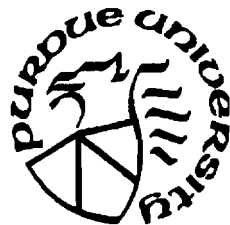
Cooper, James A. Jr., "Design Curves for Transient Heat Flow in Semiconductor Devices" (1992). *ECE Technical Reports*. Paper 284.  
<http://docs.lib.purdue.edu/ecetr/284>

This document has been made available through Purdue e-Pubs, a service of the Purdue University Libraries. Please contact [epubs@purdue.edu](mailto:epubs@purdue.edu) for additional information.

# Design Curves for Transient Heat Flow in Semiconductor Devices

**James A. Cooper, Jr.**

**TR-EE-92-9  
March, 1992**



**School of Electrical Engineering  
Purdue University  
West Lafayette, IN 47907**

**Supported by**

**Allied Signal Aerospace Corporation  
Bendix Engine Controls Division  
South Bend, IN**

**and by**

**Indiana Corporation for Science and Technology**

---

## Table of Contents

<b>Abstract</b>	<b>3</b>
<b>Introduction</b>	<b>4</b>
<b>Mathematical Formulation</b>	<b>4</b>
<b>Results</b>	<b>6</b>
<b>Summary</b>	<b>7</b>
<b>References</b>	<b>8</b>
<b>Figures</b>	<b>9</b>

---

**Abstract:**

We have **performed** a numerical simulation of heat flow in a cylindrical solid having a geometry typical of semiconductor devices. We **present** curves of temperature as a function of time, normalized to the thermal constants and the surface **heat** flux. These curves can be used in the design of **semiconductor** devices **where** transient or steady state temperature rise is a consideration.

---

## Introduction

Many **types** of semiconductor devices dissipate sufficient heat that the transient and steady state temperature extremes must be considered in the design process. Heat flow problems are treated extensively in the mathematical and mechanical engineering literature, and standard analytical and numerical techniques have been **developed** for their solution. However, the specific case of a finite heat source on a finite substrate is not treated explicitly in the **commonly** referenced texts (see, for example, refs. [1-4]). Accordingly, this geometry is analyzed herein, and the results presented in the form of normalized design **curves**.

## Mathematical Formulation

The equation governing heat flow in a solid, assuming constant **thermal** coefficients, is

$$\mathbf{K} \nabla^2 T = \rho C_p \frac{\partial T}{\partial t} \quad (1)$$

where  $\mathbf{K}$  is the thermal conductivity in (**W/cm K**),  $T$  is the absolute temperature,  $\rho$  is the density in (**g/cm<sup>3</sup>**), and  $C_p$  is the specific heat in (**J/g K**). The notation may be **simplified** by introducing normalized units. Defining

$$v = \frac{KT}{F_0 L} \quad (2)$$

$$\tau = \frac{\kappa t}{L^2}$$

where  $F_0$  is a heat flux in (**W/cm<sup>2</sup>**),  $L$  is a characteristic length in (cm), and  $\kappa = K/(\rho C_p)$  is the thermal **diffusivity** in (**cm<sup>2</sup>/s**), (1) may be written

$$L^2 \nabla^2 v = \frac{\partial v}{\partial \tau} \quad (3)$$

Specifying to cylindrical coordinates and assuming radial symmetry, so that dependences with respect to  $\theta$  are eliminated, (3) becomes

$$L^2 \left( \frac{\partial^2 v}{\partial R^2} + \frac{1}{R} \frac{\partial v}{\partial R} + \frac{\partial^2 v}{\partial Z^2} \right) = \frac{\partial v}{\partial \tau} \quad (4)$$

Defining normalized length units  $r=R/L$  and  $z=Z/L$  yields

$$\frac{\partial^2 v}{\partial r^2} + \frac{1}{r} \frac{\partial v}{\partial r} + \frac{\partial^2 v}{\partial z^2} = \frac{\partial v}{\partial \tau} \quad (5)$$

Equation (5) is to be solved subject to the boundary conditions shown in Fig. 1. We **assume** a semiconductor substrate of thickness  $L$ , mounted on a perfect heat sink. The entire structure is initially at uniform temperature  $T = 0$ . Heat is introduced into the substrate at a constant rate  $F_0$  ( $W/cm^2$ ) within radius  $R_0$  at the top surface ( $Z=0$ ). The top surface is adiabatic for  $R > R_0$ . The boundary conditions at the top surface then become

$$\frac{\partial v}{\partial z} \Big|_{z=0} = \begin{cases} 1, & r \leq r_0 \\ 0, & r > r_0 \end{cases} \quad (6)$$

and at the **bottom** surface,  $v(z=1)$  is identically zero.

Equation (5) is represented on a uniform  $(r, z, \tau)$  grid as a finite difference equation, and is solved using the explicit method [5]. The time step  $\Delta\tau$  is chosen to be

$$\Delta\tau = \frac{1}{6} \min \{ \Delta r, \Delta z \} \quad (7)$$

The **maximum**  $r$  value in the simulation,  $r = r_{\max} \gg r_0$ , is chosen in each specific situation to be large enough that the temperatures calculated **beneath** the heated region are not significantly affected. To minimize error, the radial heat flow assumed at  $r_{\max}$  is extrapolated from the heat flow at  $(r_{\max} - \Delta r)$  using a first-order Taylor series expansion.

## Results

Figure 2 shows a series of curves for the normalized temperature at  $(r=0, z=0)$  as a function of normalized time for several values of  $r_0 = R_0/L$ . These curves are shown in expanded form in Fig 3. The curve labeled  $r_0 = \infty$  is a numerical solution to the one-dimensional heat flow equation

$$\frac{\partial^2 v}{\partial z^2} = \frac{\partial v}{\partial \tau} \quad (8)$$

The solution to (8) at  $(r=0, z=0)$  can be expressed analytically when  $\tau$  is not too close to  $\pi/4$  as [1]

$$v(0,0,\tau) = \begin{cases} 2\sqrt{\frac{\tau}{\pi}} & , \tau \ll \frac{\pi}{4} \\ 1 & , \tau \gg \frac{\pi}{4} \end{cases} \quad (9a)$$

$$(9b)$$

In examining the curves in Figs. 2 and 3, we note that in the limit of small  $\tau$  the curves are independent of  $r_0$ , and the solution is given by (9a). This is because at early times in the heating transient, the heat has not reached either the edge of the heating disk at  $r = r_0$  or the heat sink at  $z = 1$ . In the limit of large  $\tau$  the temperature stabilizes (steady state). In the steady state limit, the temperature  $v(0,0,\tau)$  asymptotically approaches  $v = 1$  for  $r_0 \gg 1$  and  $v = r_0$  for  $r_0 \ll 1$ .

The transient temperature rise is presented in Figs. 2 and 3 in terms of variables normalized to the sample thickness  $L$ . It is equally informative to view the results in terms of variables normalized to the radius of the heating disk  $R_0$ . To do this, we define new normalized temperature and time variables

$$v' = \frac{KT}{F_0 R_0} = \left( \frac{L}{R_0} \right) v \quad (10)$$

$$\tau' = \frac{\kappa t}{R_0^2} = \left( \frac{L}{R_0} \right)^2 \tau$$

and plot  $v'(0,0,\tau')$  in Figs. 4 and 5 with  $r_0$  as a parameter. Here again we see that the **curves** are independent of  $r_0$  for small  $\tau'$ . In the steady state limit (large  $\tau'$ ) the **normalized** temperature  $v'(0,0,\tau')$  asymptotically approaches  $v' = 1$  for  $r_0 \gg 1$  and  $v' = 1/r_0$  for  $r_0 \ll 1$ .

In Figs. 4 and 5 we note that the curves for  $r_0 \ll 1$  are virtually identical, so that curves for  $r_0 < 0.1$  may be generated by scaling the  $r_0 = 0.1$  **curve**. This is confirmed in Fig. 6, where the curve computed numerically for  $r_0 = 0.05$  is compared with the scaled  $r_0 = 0.1$  curve. In like manner, it follows from the close agreement between the  $r_0 = 5$  and  $r_0 = \infty$  curves in Fig. 3 that new curves for  $r_0 > 5$  may be generated by scaling the  $r_0 = \infty$  curve. Figure 7 shows the computed curve for  $r_0 = 5$  compared with the scaled  $r_0 = \infty$  curve. This scaling technique **was** actually used in Fig. 4 to produce the curves for  $r_0 = 10$  and  $r_0 = 20$ .

The curves in Figs. 2-5 provide the transient temperature rise at the center of a circular heating disk of various radii on a substrate of finite thickness. While this represents the greatest temperature rise in the structure, and is thus a worst case condition, it may also be of interest to know the temperature distribution along the top **surface** and axially beneath the heating disk in steady state. These **distributions** are shown in Figs. 8 and 9. From Fig. 9 we observe that for  $r_0 \gg 1$ , the heat flow is primarily axial, leading to a linear variation in temperature with depth in steady state. For  $r_0 \ll 1$ , the gradient of temperature approaches zero for  $z \approx 1$ , indicating that heat flow is primarily in the radial direction.

## Summary

In summary, we have performed a numerical simulation of the transient heat flow in a cylindrical solid of finite thickness and infinite radius, where heat is supplied at the top surface from a heating disk of finite radius and sunk at the bottom surface into a heat sink of infinite radius. This geometry is typical of most semiconductor device applications. We have presented **curves** showing **temperature** at the center of the heating disk, normalized to the **thermal** constants and the **surface** heat flux. These curves can be used in **the** design of **semiconductor** devices where transient or steady state temperature rise is a consideration.

---

## References

- [1] **H. S. Carslaw** and J. C. Jaeger, "Conduction of Heat in Solids," 2<sup>nd</sup> Ed., **Clarendon** Press, Oxford, 1959.
  - [2] **F. P. Incropera** and D. P. **DeWitt**, "Fundamentals of Heat and Mass Transfer," 3<sup>rd</sup> Ed., John Wiley & Sons, New York, 1990.
  - [3] **S. Kakac** and Y. Yener, "Heat Conduction," 2<sup>nd</sup> Ed., Hemisphere Publishing **Corp.**, Washington, 1985.
  - [4] M. N. Ozisik, "Heat Transfer: A Basic Approach," **McGraw-Hill**, New York, 1985..
  - [5] **B. Carnahan**, H. A. Luther, and J. **O. Wilkes**, "Applied Numerical Methods," John Wiley & Sons, New York, 1969.
- 
-

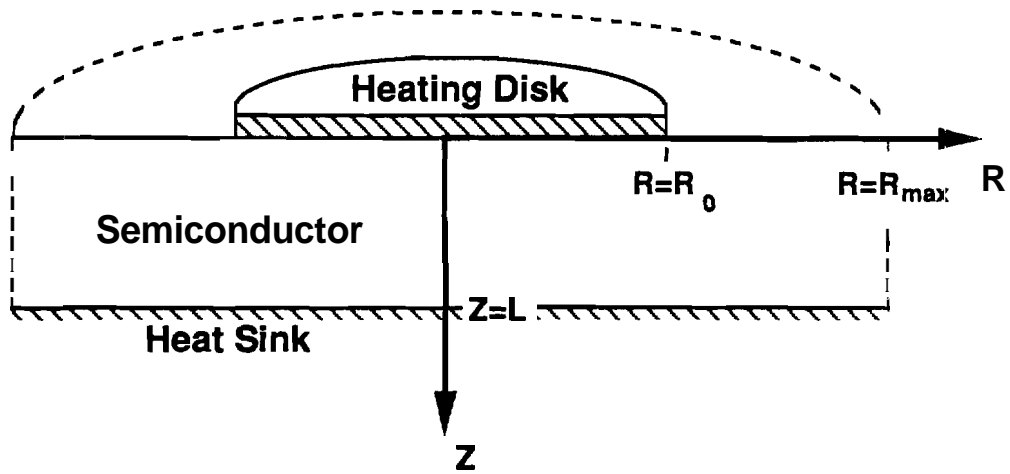


Figure 1. Geometry used to simulate transient heat flow in semiconductor devices. Heat is introduced uniformly at the top surface by a heating disk of radius  $R_0$ , and the bottom surface is mounted on a perfect heat sink.

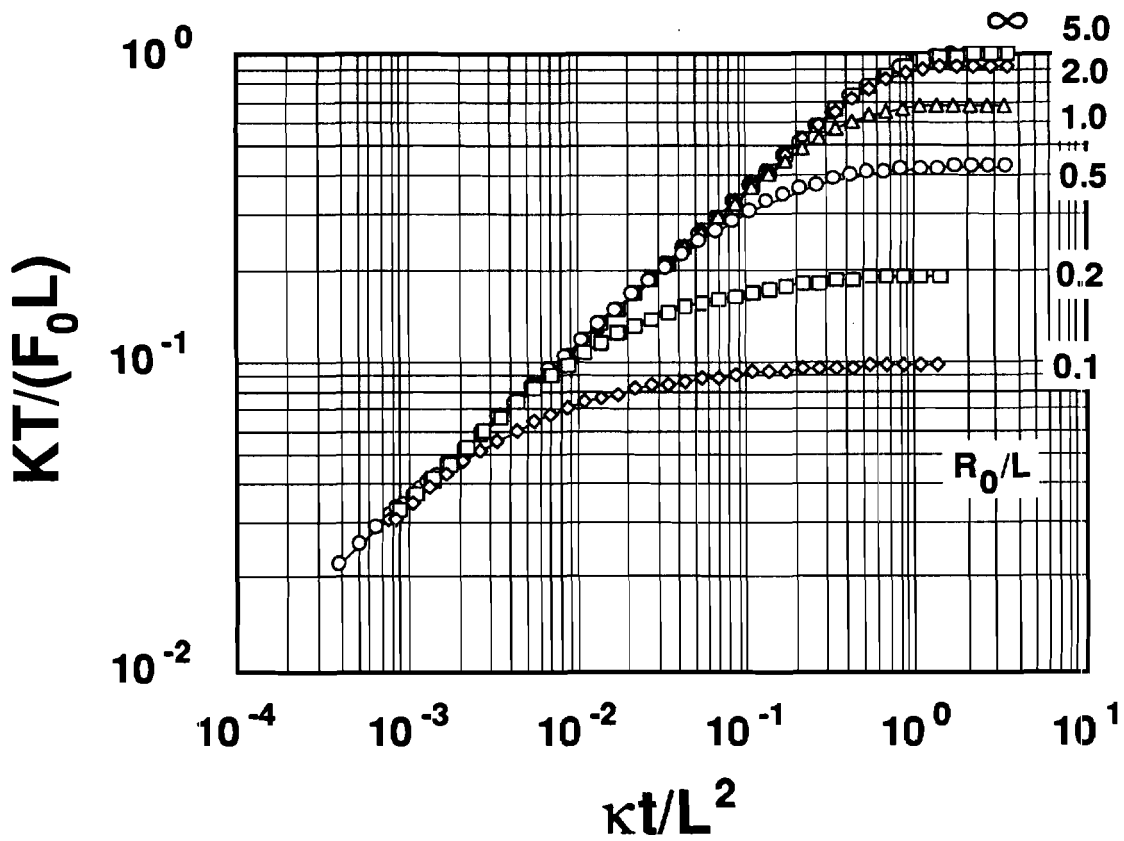


Figure 2. Temperature at the center of the heating disk ( $R=0, Z=0$ ) as a function of time for several radii  $R_0$ . The temperature and time variables are normalized to  $L$ .

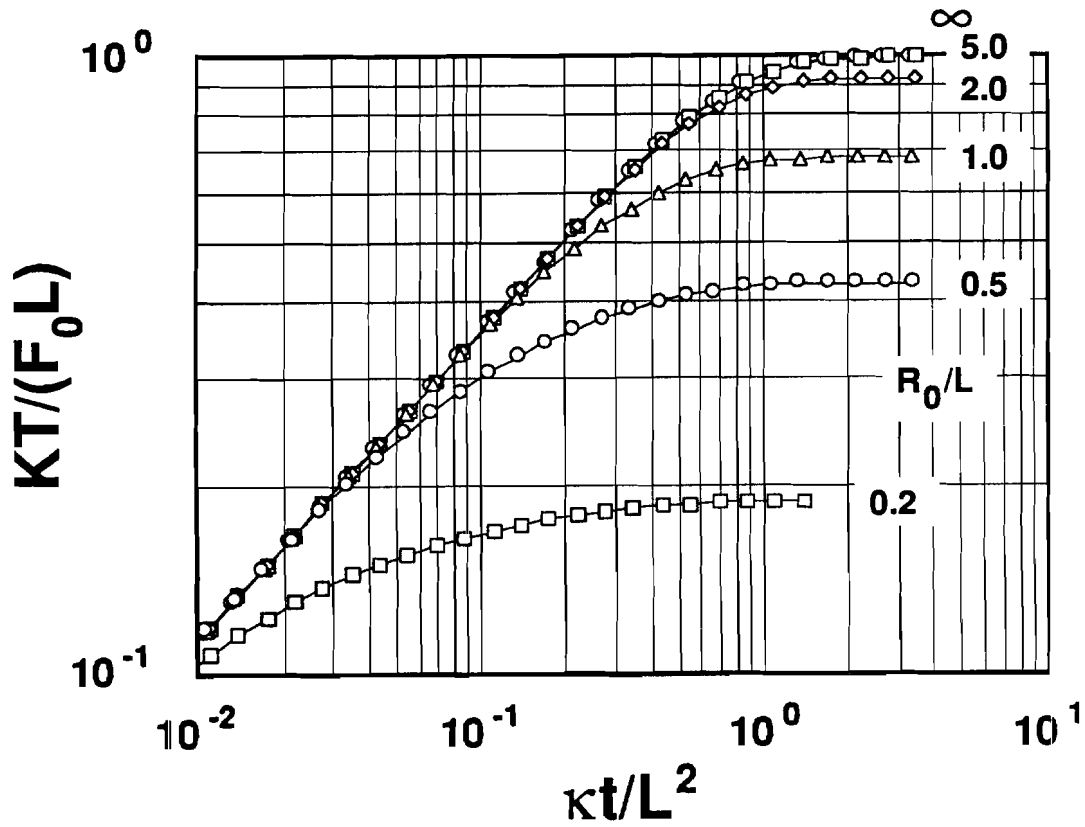


Figure 3. Temperature at the center of the heating disk ( $R=0, Z=0$ ) as a function of time for several radii  $R_0$ , showing the region  $KT/(F_0L) > 0.1$  in greater detail.

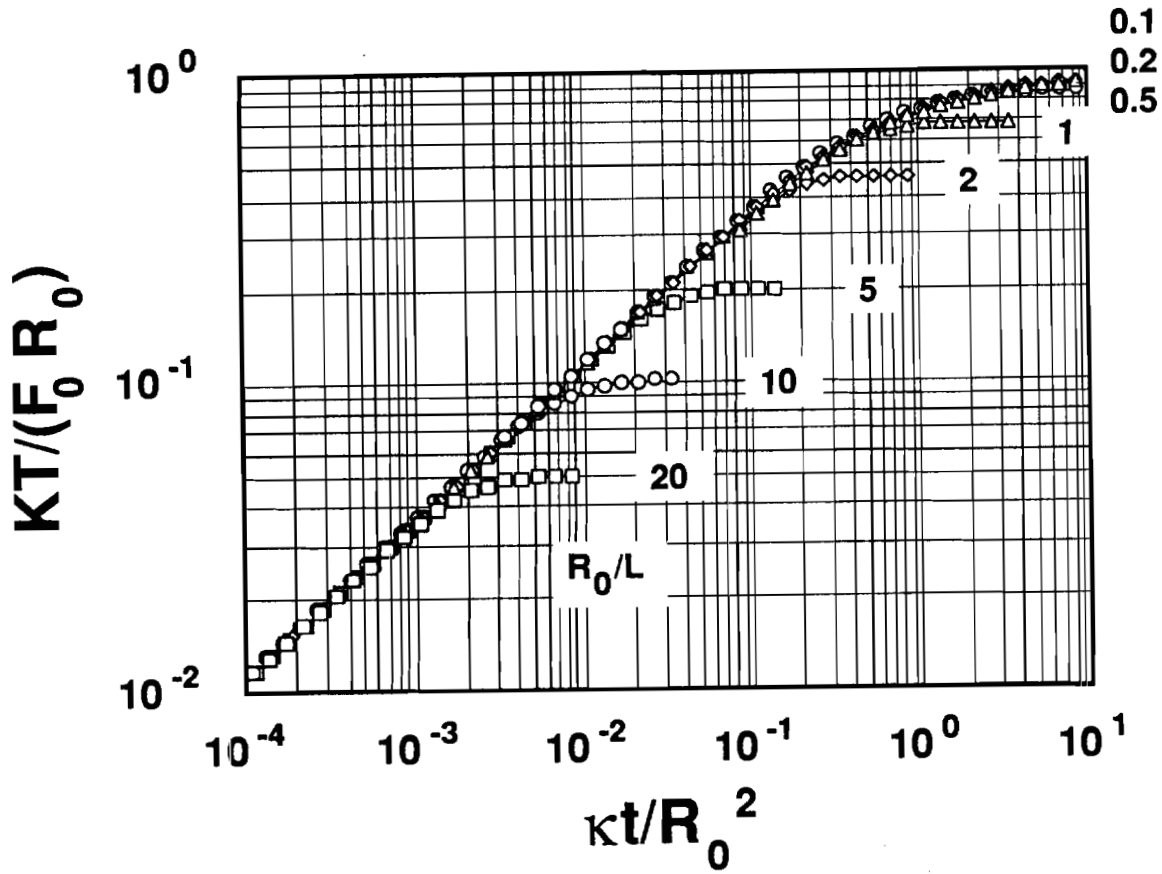


Figure 4. Temperature at the center of the heating disk ( $R=0, Z=0$ ) as a function of time for several radii  $R_0$ . The temperature and time variables are normalized to  $R_0$ .

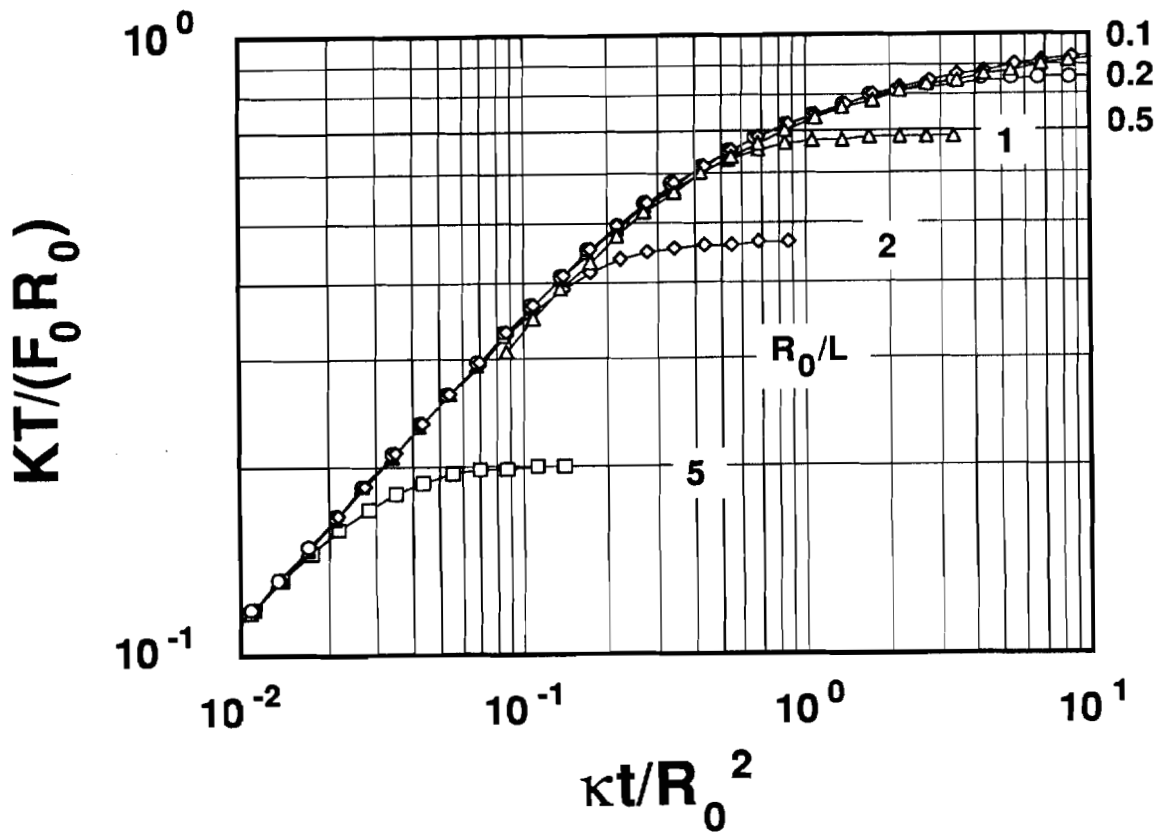


Figure 5. Temperature at the center of the heating disk ( $R=0$ ,  $Z=0$ ) as a function of time for several radii  $R_0$ , showing the region  $KT/(F_0R_0) > 0.1$  in greater detail.

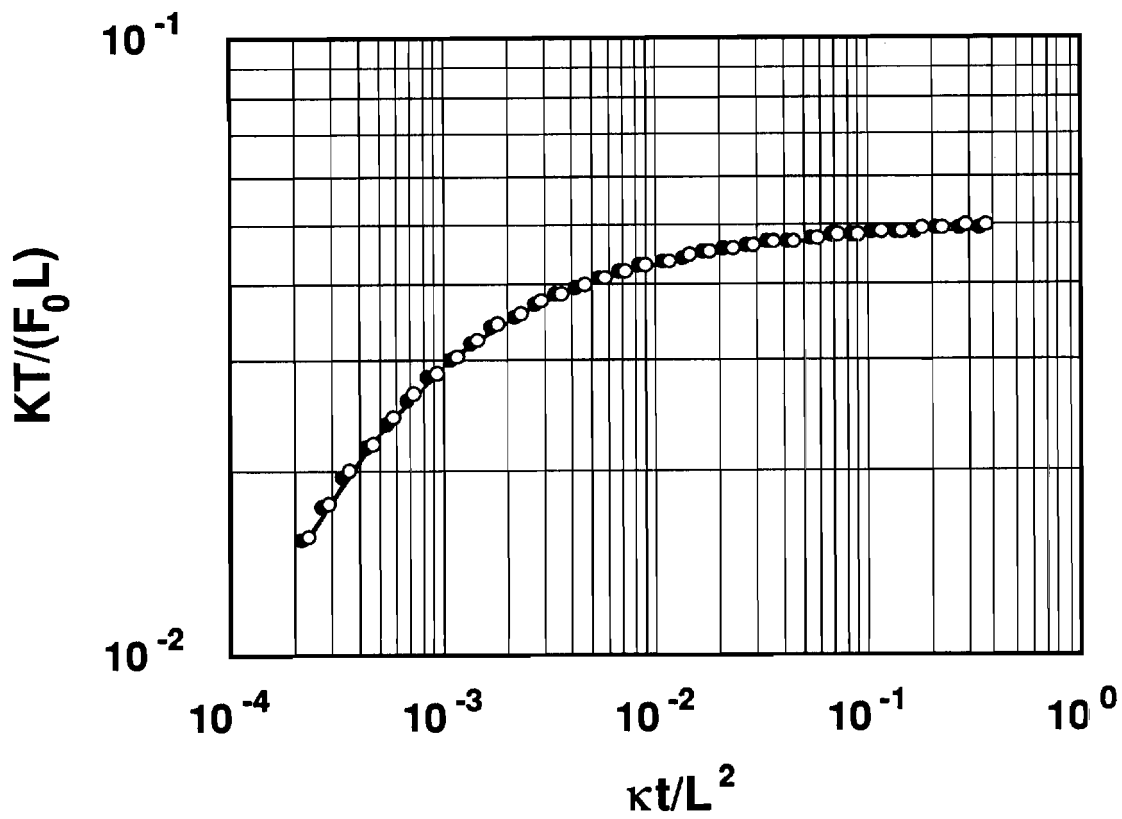


Figure 6. Temperature versus time for  $R_0/L = 0.05$ . The open circles are computed for this geometry and the closed circles are obtained by scaling the curve for  $R_0/L = 0.1$ .

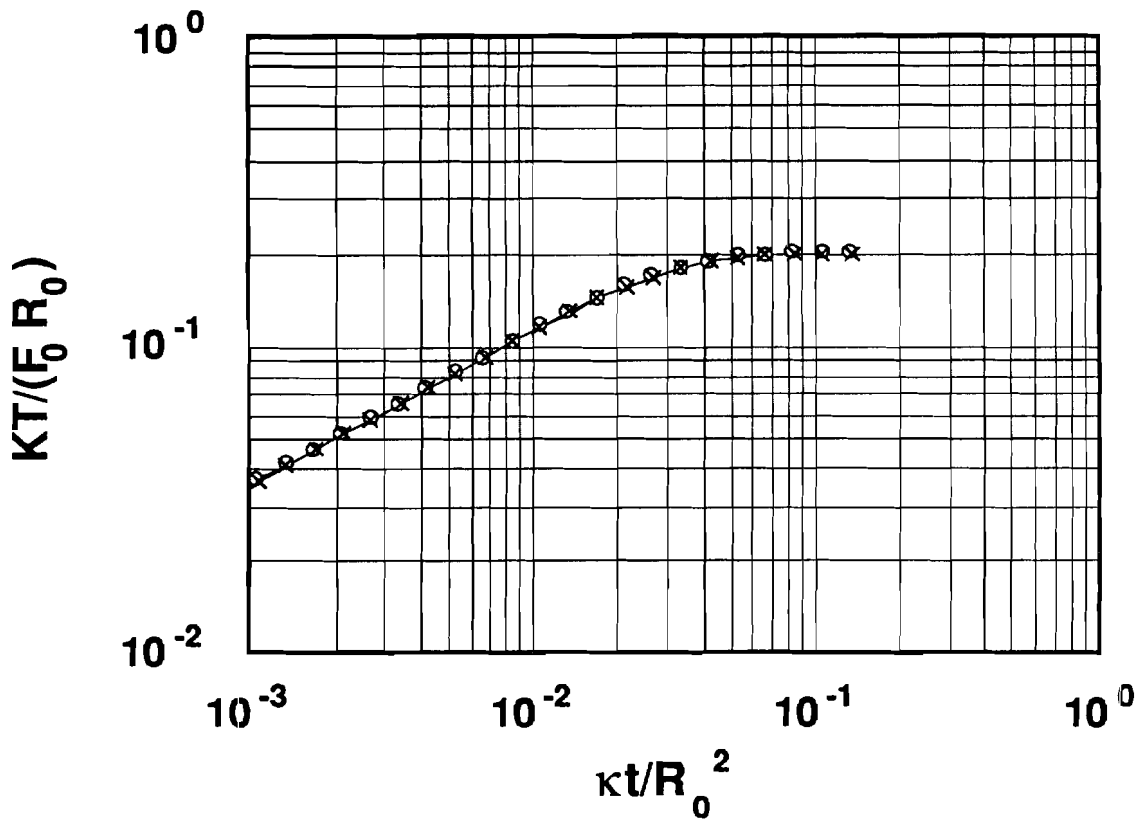


Figure 7. Temperature versus time for  $R_0/L = 5$ . The crosses are computed for this geometry and the circles are obtained by scaling the curve for  $R_0/L = \infty$ .

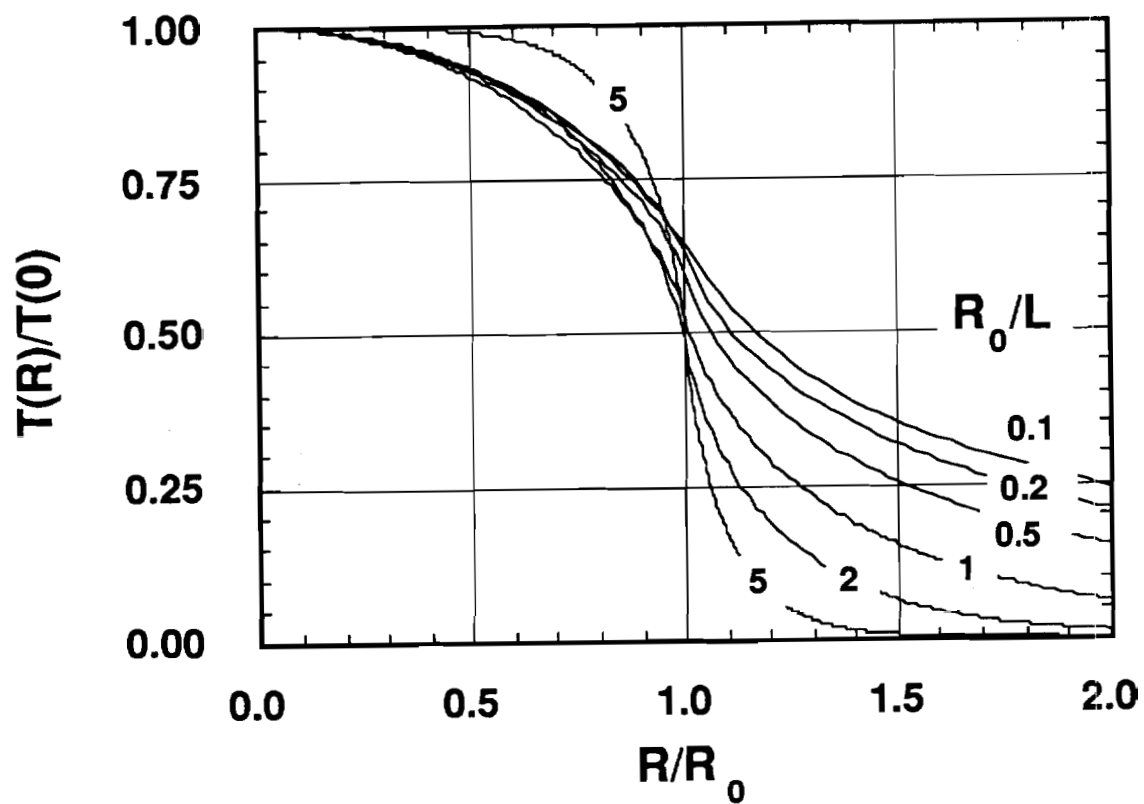


Figure 8. Temperature at the top surface ( $Z=0$ ) versus radial position in steady state.

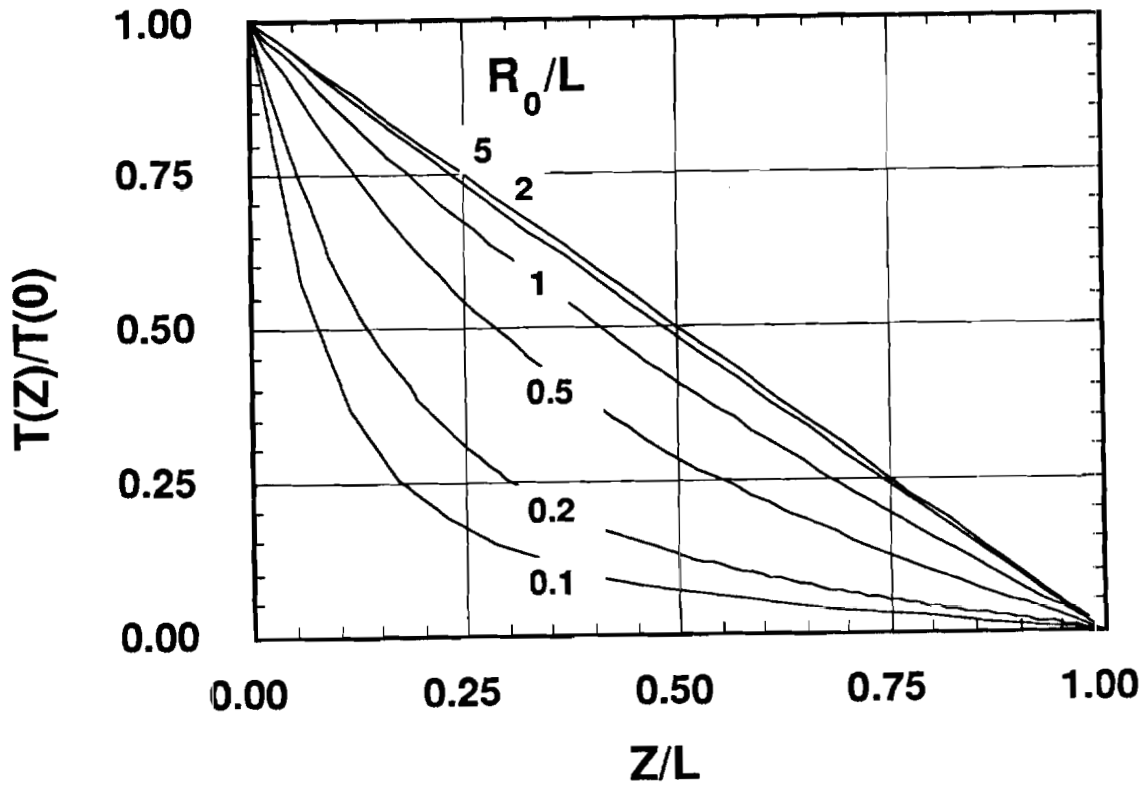


Figure 9. Temperature along the central axis ( $R=0$ ) versus depth in steady state.